

## **General Disclaimer**

### **One or more of the Following Statements may affect this Document**

- This document has been reproduced from the best copy furnished by the organizational source. It is being released in the interest of making available as much information as possible.
- This document may contain data, which exceeds the sheet parameters. It was furnished in this condition by the organizational source and is the best copy available.
- This document may contain tone-on-tone or color graphs, charts and/or pictures, which have been reproduced in black and white.
- This document is paginated as submitted by the original source.
- Portions of this document are not fully legible due to the historical nature of some of the material. However, it is the best reproduction available from the original submission.

091418

THE STRUCTURE OF THE PLASMA SHEET - LOBE BOUNDARY  
IN THE EARTH'S MAGNETOTAIL

S.Orsini, M.Candidi, V.Formisano  
H.Balsiger, A.Ghielmetti, K.W.Ogilvie

IFSI-82-9

September 1982

RECEIVED BY  
ESA - SDS 30 SET. 1983  
DATE:  
DCAF NO. 320109  
PROCESSED BY  
 NASA STI FACILITY  
 ESA - SDS  AIAA

ISTITUTO  
DI FISICA DELLO SPAZIO INTERPLANETARIO  
CONSIGLIO NAZIONALE DELLE RICERCHE  
VIA G. GALILEI — 03044 FRASCATI (ITALIA)

THE STRUCTURE OF THE PLASMA SHEET - LOBE BOUNDARY  
IN THE EARTH'S MAGNETOTAIL

S.Orsini<sup>\*</sup>, M.Candidi<sup>\*\*</sup>, V.Formisano

Istituto di Fisica dello Spazio Interplanetario, CNR,  
00044 Frascati (Rome), Italy

H.Balsiger, A.Ghielmetti

Physikalisches Institut, University of Bern (Switzerland)

K.W.Ogilvie

Laboratory for Extraterrestrial Physics, Goddard Space Flight Center,  
Greenbelt MD 20771, USA

*original contains color illustrations*

\*) currently at Physikalisches Institut, University of Bern (Switzerland).

\*\*) currently at Applied Physics Lab., Johns Hopkins University, Laurel Maryland 20810, USA.

ABSTRACT. The structure of the magnetotail plasma sheet-plasma lobe boundary is studied by observing the properties of tailward flowing  $O^+$  ion beams, which have been detected by the ISEE-2 plasma experiment inside the boundary during three time periods on April 1978. The computed value of the north-south electric field component as well as the  $O^+$  parameters are shown to change at the boundary. The results are discussed and related to the other observations made in this region. The  $O^+$  parameters and the  $E_z$  component behaviour are shown to be consistent with that expected from the topology of the electric field lines in the tail as mapped from the ionosphere.

#### INTRODUCTION

Studies have been conducted that show substantial differences between the inner region and the outer layer of the plasma sheet, at the interface with the magnetotail plasma lobes. As regards the thermal plasma, Lui et al. (1977) have published data from IMP-6 for various substorms in 1971-1972; they show that the earthward flow of protons, in the 50 eV/charge to 40 keV/charge range, has a higher velocity close to the outer plasma sheet boundary than in the inner plasma sheet, in the  $R < 30 R_E$  region. De Coster and Frank (1979) report similar observations using IMP 7 and 8 proton data for 1975-1976, for the region at distances between 30 and 40  $R_E$  in the tail in the same energy/charge interval; they suggest that this earthward flowing plasma is responsible for the thickening of the plasma sheet after the substorm thinning; they estimate a North-South velocity for the surface of the expanding plasma sheet of about 11 km/s. Parks et al. (1979) report the observation at 1.5, 6 and  $> 16$  keV, of an energetic non-thermal electron and ion layer a few thousand km thick, right outside the plasma sheet boundary, at 20  $R_E$ . Multiple layers of flowing electrons and protons have been detected by the ISEE satellites at 20  $R_E$  (Frank et al., 1981) and

it has been shown that these flows carry electric currents on the plasma sheet surface. As for the particles at higher energy, Spjeldvik and Fritz (1981) have presented ISEE-1 data in the 25 keV to 445 keV range that show ions and electrons flowing at the surface of the plasma sheet, during substorm activity on March 24, 1978, around  $X_{SE} = -15$  to  $-20 R_E$  locations. From the detailed observation of a multiple encounter with this layer of flowing plasma they infer either a multiple structure or a wave-like modulation of the plasma sheet boundary surface. Andrews et al. (1981) have observed, on ISEE-2 at  $\sim 15 R_E$ , a structured layer of ions between 25 keV and 2.5 MeV jetting towards the Earth at the plasma sheet boundary, together with the tailward return flow of mirroring ions. The energy dispersion characteristics of these ions are explained as the effects of their flow in the magnetotail  $\underline{E}$  field and of the motion of their source. Similar observations are reported by D.J. Williams (1981).

Streams of cold  $O^+$  ions flowing tailwards, with energies in the order of hundreds of eV, have been detected in the northern magnetotail plasma lobe and, at times, within the plasma sheet (Sharp et al., 1981; Orsini et al., 1982; Candidi et al., 1982). Hot  $O^+$  in the energy range 1 to 17 keV is sometimes the major constituent of the plasma sheet (Peterson et al., 1981). The  $\underline{E} \times \underline{B}$  drift in the plasma lobes has been suggested as a possible mechanism by which the  $O^+$  ion streams are driven towards the plasma sheet; after being energized and thermalized these  $O^+$  ions could become part of the plasma sheet (Pilipp and Morfill, 1976).

In the following we will report on the observation of  $O^+$  ion streams at the boundary between the lobes and the plasma sheet and on the modifications of properties at the transition. The structure of the boundary itself will be investigated by using the  $O^+$  ions as test particles.

## INSTRUMENTATION AND DATA BASE

The description of the ISEE-2 plasma experiment (PE) was given in Bonifazi et al. (1978). Here it will be sufficient to recall that it counts positive ions travelling within  $\pm 45^\circ$  of the satellite equatorial plane (i.e. within nearly  $\pm 45^\circ$  of the SE equatorial plane), in the energy/charge range 400 eV/q to 4.0 keV/q in steps of  $\Delta E/E \sim 4\%$ , with additional measurements at 56, 86, 155 and 240 eV/q and at 5.43, 7.03, 8.37 and 10.3 keV/q. The angular resolution in the equatorial plane is  $5.6^\circ$  (or  $2.8^\circ$  in high bit rate) for the  $68^\circ$  sector centered at the Sun direction (i.e. for tailward flowing ions) and  $90^\circ$  (or  $45^\circ$  in high bit rate) for the other three  $90^\circ$  sectors. A  $22.8^\circ$  blind sector is present between the tailward flow and the duskward flow sectors. One complete distribution (in energy and in angle) is sampled every 96 seconds.

For this study five periods of continuous observation, totalling 37.5 hours, have been selected. For all these periods the identification of the  $O^+$  ions has been made with the ISEE-1 ion composition experiment (ICE) data. Details about the identification of the ion species for the selected plasma sheet periods will be given. The corresponding observations during the lobe periods have been discussed in Orsini et al. (1982). Lobe and plasma sheet samples are present in the data set during geomagnetically active times.

Event A: Days 113-114; April 23, 2000 UT to April 24, 0800 UT, 1978.

The satellite pair travels in the tail between  $X_{SE} = -19 R_E$  and  $X_{SE} = -14 R_E$  ( $Y_{SE}$  between 7 and  $3 R_E$  and  $Z_{SE}$  between 6 and  $8 R_E$ ). The PE energy spectra for the tailward flow and for the earthward flow sectors are shown in the 3D plots of Figure 1. Particles, at energies above 1 keV, are present between 0000 UT and 0130 UT, between 0335 and 0500 UT and between 0605 UT and 0800 UT. This plasma is nearly isotro-

pic (it is present in both flow directions). These features are typical for the plasma sheet population. At low energy, in the tailward flow sector only, a population is present at times, both in the lobe region as well as within the plasma-sheet.

To assess the nature of these low energy ions, data from the ISEE-2 PE and from the ISEE-1 ICE were compared. The differential fluxes measured by the two experiments have been averaged over one hour and are shown, as an example, in Figure 2 (0300-0400 UT day 114). It shows that, both in the tailward flow and the earthward flow sectors, protons are the dominant ions of the plasma sheet, at energies above 1 keV. At energies below 1 keV the ICE data reveal that tailward flowing  $O^+$  fluxes are almost 3-5 times higher than  $H^+$  fluxes. Since the PE data show high fluxes of ions flowing tailwards in this energy range, these are identified as  $O^+$ . The differences between the  $O^+$  fluxes as measured by the two instruments probably result from sampling effect, since the ICE time coverage is not continuous.

Quantitative analysis of the PE  $O^+$  data have been performed; the derived parameters for the interval 2300 UT day 113, 0700 UT day 114 are plotted versus time in Figure 3 together with the computed north-south component of the electric field:

$$E_z = v_{Dx} B_y - v_{Dy} B_x$$

where  $v_{Dx}$  and  $v_{Dy}$  are the  $O^+$  ions drift velocity components on the SE equatorial plane;  $B_x$  and  $B_y$  are the ISEE-2 magnetic field components on the same plane (Russell, 1978).

The top panels represent the ISEE-1 electron spectrometer 724 eV measurements and the ISEE-2 plasma experiment 5-10 keV positive ion count rates. These two plots show the presence/absence of the plasma

sheet particles. When the satellite moves from the plasma sheet into the lobes, the plasma sheet proton signal disappears earlier at low energies than at higher energies. The disagreement between the proton and electron detection of the plasma sheet could be due to the 11 keV energy upper limit of the PE. The plasma sheet ions near the boundary couldn't be detected because of their too high energy. This is confirmed by the presence of high energy protons when the satellites were crossing the boundary on day 114, around 0320 UT (Spieldvjk and Fritz, 1981). The first signal, at ISEE-1, occurs at 0316 UT, well before the low energy protons are detected at ISEE-2, around 0335 UT. The separation between ISEE 1 and 2 (250 km, and only a few km in  $Z_{SM}$ ) cannot explain this delay.

The tailward streaming  $O^+$  ion parameters are plotted in the lower panels. They reveal several noticeable features. The density shows maxima around 2340 UT, around 0200 UT, at 0315 UT and at 0500 UT. These maxima generally occur at times when the electron spectrometer signal is wiggling above background. It should be noted that the peak at 0315 UT occurs when the high energy earthward streaming protons are observed (Spieldvjk and Fritz, 1981). A decrease in the  $O^+$  bulk flow velocity is also evident at the same times.

The middle panel of Figure 3 shows the time evolution of  $E_z$ , the vertical component of the ambient electric field. This has been computed by assuming that the bulk flow velocity of the ions always lies in the SE XY plane ( $\underline{V} \equiv \underline{V}_{xy}$ ); this can introduce an overestimate of  $|E_z|$  by a maximum of 25% (no change in sign can be introduced by this assumption). It can be seen in the figure that  $E_z$  changes polarity when the peak in density appears.

All the features mentioned are shown in the angular distributions of Figure 4. This is a sequence of four contiguous  $96 \text{ s } V_x V_y$  ( $H^+$  equivalent) scans of the differential fluxes as computed by the PE data between 0312 and 0317 UT, day 114. Only tailward flow sector fluxes are

shown, since no signal is detected in other directions. In the 1<sup>st</sup> panel the intense  $O^+$  beam is very cold and collimated. When the density increases (2<sup>nd</sup> panel) the flow direction reverses and the velocity looks like to decrease.

Event B: day 100, April 10, 1600 to 2400 UT, 1978;  
day 101, April 11, 0800 to 1200 UT, 1978.

The orbit segment for this event extends between  $X_{SE} = -12 R_E$  and  $X_{SE} = -20.5 R_E$  ( $Y_{SE}$  between  $7.5$  and  $5 R_E$ ;  $Z_{SE}$  between  $5.50$  and  $8 R_E$ ).

Figure 5 shows a 3D plot of the plasma experiment data; the same features as for event A are noticeable, with plasma sheet detection between 1600 UT and 1700 UT, between 1800 UT and 1905 UT, and between 1940 UT and 2150 UT, the low energy peak has a higher intensity and is more persistent in this case. As an example, the comparison with the ICE data is shown in Figure 6, for the hourly average between 1800 UT and 1900 UT, day 100. The plasma sheet-like population (isotropic) is composed essentially of  $H^+$ , whereas the tailward flowing cold ions at energies below 1 keV are made up primarily of  $O^+$  (ICE protons <1 keV are below the plasma experiment one count threshold in that range).

Figure 7 shows the  $O^+$  ion stream parameters derived by the PE data plotted versus time and the energetic protons and electrons count rates for the period 1600-2300 UT, day 100. In this time period a lobe observation can be defined only after 2220 UT (there is a gap in the electron spectrometer data between 2120 UT and 2220 UT). Before 2120 UT (and after 1600 UT) the 219 eV electron count rate is always above background. The satellites are apparently moving from the plasma sheet to the boundary region, where the ion count rate goes to zero, but do not reach the lobes before the data gap. For this reason it is harder to interpret the time behaviour of the  $O^+$  ion stream density and flow direction; these parameters display frequent fluctuations as if the location of the density maximum and drift reversal were traversed

several times. The estimated  $E_z$ , computed under the usual assumptions, shows several variations. It should be noted that the  $E_z$  computed value may be inferred by temporal fluctuations or by too large angular spreads, especially when the  $O^+$  density is low.

Event C: day 103, April 13, 2000 to 2400 UT, 1978;

day 104, April 14, 0430 to 1100 UT, 1978.

The satellites move between  $X_{SE} = -20$  and  $-18 R_E$  (with  $Y_{SE} = 6$  to  $1.5$  and  $Z_{SE} = 8$  to  $6.5$ ). The ISEE-2 PE 3D plots are shown in Figure 8. The plasma sheet signal is detected between 2000 and 2042 UT on day 103 and between 0830 and 1000 UT, on day 104. A consistent  $O^+$  ion stream is often observed in the tailward flow sector during the whole two periods. The identification of  $O^+$  is based on ISEE-1 ICE data: Figure 9 (analogous to figures 2 and 6) refers to the hourly average between 0830 and 0930 UT on day 104. The  $O^+$  flux measured by ICE is from 4 to 10 times higher than the proton flux, below 1 keV, where the plasma experiment detects the tailward streaming particles, which we therefore identify as  $O^+$ . Protons are in fact below the ISEE-2 plasma experiment sensitivity threshold in that energy range.

The plots of the  $O^+$  parameters together with the computed  $E_z$  and the 724 eV electron spectrometer data are shown in Figure 10, for the period 2100-2400 UT, day 103. No positive ions are detected in the 5-10 keV energy range. The ISEE-1 electron spectrometer shows plasma sheet electrons at times, between 2100 UT and 2150 UT; after 2150 UT the spacecrafts are in the lobe. When the electrons are present, their flux is highly variable; the satellites are in the boundary region before 2150 UT, where they move towards the plasma sheet and recover as they move towards the lobe, which they enter at 2150 UT. The  $O^+$  density is too low before 2120 UT to be analyzed, but during the final excursion,

2120-2150 UT, it increases and the typical behaviour of the flow velocity direction is seen, with double reversal at 2128 and 2132 UT (no peak in density is present here) and a final deflection to zero at 2205 UT in association with a density increase.

### STATISTICAL ANALYSIS

Three different regions have been defined on the basis of the presence or absence of plasma sheet signal in the ISEE-2 plasma experiment and in the ISEE-1 electron spectrometer data. When both instruments detect particles in the two selected energy ranges we define a "plasma sheet" observation; when both show no flux above background ( $\sim 10^3 \text{ cm}^{-2} \text{ s}^{-1} \text{ sr}^{-1} \text{ keV}^{-1}$ ) we define a "lobe" observation; when electrons are present, but no signal is seen in the protons a "boundary region" observation is defined.

The overall 37.5 hours of data from the plasma experiment have been analysed statistically, as regards the parameters of the  $O^+$  ion streams (Figure 11). A lower limit of  $2 \cdot 10^{-3} \text{ cm}^{-3}$  (corresponding to  $\sim 10^5 \text{ cm}^{-2} \text{ s}^{-1} \text{ sr}^{-1} \text{ keV}^{-1}$ ) on the density has been chosen for confidence in the derived parameters. When the plasma sheet signal was observed, 3 counts per angular subsector ( $5.6^\circ$  or  $2.8^\circ$  depending on bit rate) were subtracted in the tailward flow sector, to account for the low energy tail of the plasma sheet protons. This drastically cut our data base to about 300, 100 and 80 spectra for lobes, boundary and plasma sheet respectively. The right upper panel of Figure 11 shows the  $YZ_{SM}$  plane projection of the ISEE satellite locations at which the measurements were taken. The other panels show the statistics over the  $O^+$  parameters and the computed  $E_z$  value. The average values of the histograms are shown in table 1.

Averages	P. Sheet	Boundary	Lobe
$O^+$ density ( $cm^{-3}$ )	0.08	0.18	0.13
$O^+$ velocity (km/s)	67	46	64
Computed $E_z$ (mV/m)	-.56	-.54	-.11

Table 1. Average values from the histograms of Figure 11.

The density of the  $O^+$  ion streams seems to be higher in the boundary region (where the density peaks are observed) than in the lobe/plasma sheet regions and the  $O^+$  velocity appears to be lower. The thermal velocity is generally higher in the plasma sheet than in the other regions, with the usual anisotropy, the perpendicular thermal velocity being in a ratio of 2 or 3 to the parallel thermal velocity (Candidi et al., 1982). The computed north-south electric field value appears to be more frequently negative in the boundary and plasma sheet regions than in the lobes. This result is in agreement with the single events observation.

#### DISCUSSION

The properties of the  $O^+$  ion streams inside the plasma sheet have been investigated by Sharp et al. (1981) using a data set much larger than the one used for this study. Furthermore we have intentionally limited our attention to periods when the ISEE satellites were presumably close to the plasma sheet boundary. Nevertheless the heating of the  $O^+$  beams into the plasma sheet that result from our analysis is in agreement with their conclusions.

In the boundary region, the computed density of  $O^+$  ions appears somewhat higher than elsewhere; whereas the  $O^+$  density distributions in the lobes and in the plasma sheet are similar (in agreement with Sharp et al., 1981). The bulk flow velocity in the boundary region is distributed around values lower than in the lobes and in the plasma sheet. These statistical results can be noticed in the individual cases, as shown in Table 2.

UT	Dens ( $cm^{-3}$ )	before/after	Vel (km/s)	before/after
100 1710-1730	.34	.15/.04	30	53/65
100 1900-1930	.28	.17/.09	36	51/60
103 2130-2215	.11	- /.06	58	- /72
114 0159-0205	.27	.20/.08	42	48/53
114 0314-0315	.90	.05/.01	53	68/68

Table 2.  $O^+$  average parameters for 5 boundary crosses. Values of time equivalent contiguous periods are shown for comparison.

In coincidence with the density maxima in the  $O^+$  ion streams, we see dips in the flow velocity trace, around 0200 and 0315, day 114, and a lower velocity period around 0500-0530 UT, when the density is generally high (see Figure 3). The density peaks at 1710-1730 UT and 1900-1930 UT, day 100, are generally associated with lower velocity (Figure 7). The  $E_z$  reversal around 2130-2215 UT, day 103, is associated with velocity lower than afterwards, in the lobe (Figure 10).

The position of the satellite at the time the measurements were made was roughly in the central magnetotail. Furthermore the direction of  $\underline{B}$ , with  $B_y$  generally positive, indicates that we are located for most of the time on the dawn side of the magnetotail. The mapping

of the ionospheric electric fields into the magnetotail (Rostoker and Bostrom, 1976) predicts an inversion of the ambient electric field when crossing into the plasma sheet. The reversal of flow that is observed in the polar ionosphere when the auroral oval is traversed (see Fairfield, 1977, for a review) is interpreted in terms of an electric field reversal. As a matter of fact the XY component of the flow, when ISEE-2 crosses between lobe and plasma sheet in the magnetotail appears to change its sign as well. This should be interpreted there again as a reversal of polarity of the ambient electric field.

Fig. 12a and 12b refer to another plasma sheet boundary crossing on March 22 1979 around 1453 UT. Eight  $v_x - v_y$  ( $H^+$  equivalent) angular distributions of the differential energy fluxes are shown. The crossing of the boundary occurred when the instrument was operating in the high time resolution mode. This particular mode of operation only scans the energy channels that are close to those with the maximum count rate; the measurements are therefore taken at few seconds time resolution, but energy coverage is reduced. In Figure 12a the four panels show the typical lobe  $O^+$  ions. The first panel is a normal operation 96 s mode angular distribution for all flow directions (only a low energy, intense and collimated beam is distinguishable). The other three plots are obtained from the high time resolution mode data and show the tailward flowing beam present before 1453 UT. At that time the ISEE-1 electron spectrometer 724 eV count rates (not presented here) increase to the typical plasma sheet values, thus indicating that the satellites are crossing the plasma sheet boundary. In this particular case the satellites are entering the plasma sheet from the southern lobe, on the dawn magnetotail side. Figure 12b represents four angular distributions detected after 1453 UT. The first three are taken in the high time resolution mode and detect at the  $O^+$  beams (inside the plasma sheet). The last one is a complete overview of the data over 96 seconds, obtained some minutes later: the typical plasma sheet population

is present, characterized by energetic and nearly isotropic fluxes with the maximum in the earthward flow sector, superimposed to the low energy highly fluctuating  $O^+$  beam.

The high time resolution demonstrates the sharpness of the transition. On a time scale of a few seconds, the direction of the drift reverses from dawn-to-dusk in the lobe (i.e. positive  $E_z$ ) to dusk-to-dawn in the plasma sheet. The decrease of the  $O^+$  ion stream velocity around 1452<sup>53</sup> UT is evident and the drift velocity is already lower in that panel, an indication of the beginning of the flow reversal. The decrease in the bulk flow velocity can be explained, using the Rostoker and Bostrom model, by the traversal, at the time of the crossing, of a positively charged layer that should be present, according to that model, on the plasma sheet surface on the dawn side. The  $O^+$  ions would be slowed down when approaching the charged layer and accelerated to their initial energy as they recede from it. The possibility that this decrease could be due to an increase of the north-south component of the flow velocity, so that part of the signal could have been lost due to the plasma experiment  $\pm 45^\circ$  latitude cut-off, is not in agreement with the contemporary increase of the density, that could imply a concentration of low-velocity  $O^+$  in the boundary region. On the other hand, the rapid evolution of the ion velocity and direction suggest that the instrument, when operating in the normal 96 seconds mode of operation, might have detected the  $O^+$  beam more than once in a single spectrum, thus increasing the computed value for the density.

#### SUMMARY AND CONCLUSIONS

We have studied the structure of the plasma sheet - plasma lobe boundary in the magnetotail as observed by some experiments on board the ISEE satellites during three events in 1978. The parameters of the  $O^+$  ion beams (identified by the ISEE-1 ICE), as computed by the ISEE-2

plasma experiment, have been used together with the ISEE-2 magnetic field data to calculate the north-south DC electric field component. By looking at the presence or absence of the 5-10 keV positive ions and of the 219 eV and 724 eV electrons we have defined three regions, named "plasma sheet", "boundary" and "lobe".

It has been shown that in the boundary region:

- 1) The  $O^+$  density increases. In one case (day 114, 0317 UT) this increase occurs together with the observation of an intense high energy  $H^+$  beam flowing earthwards (Spjeldvik and Fritz, 1981);
- 2) The  $O^+$  bulk flow velocity decreases;
- 3) The  $O^+$  flow direction changes its sign, so that the computed  $E_z$  behaviour is in agreement with the magnetotail electric field configuration as modeled by Rostoker and Bostrom (1976).

The angular distributions in a  $V_x - V_y$  SE plane for another time period (1979, day 81, 1450-1500 UT), when the ISEE-2 plasma experiment was operating in the high time resolution mode, shows that the flow direction reversal occurs abruptly, in a few seconds. It has been shown that the abrupt decrease of the beam bulk flow velocity occurs during the boundary crossing, as if a positively charged layer was encountered.

Acknowledgements: Part of this work was supported by the Swiss National Foundation.

Dr. C.T. Russell of UCLA has provided the ISEE-2 magnetometer data.

## REFERENCES

- Andrews, M. K., P. W. Daly, E. Keppler, Ion jetting at the plasma sheet boundary: simultaneous observations of incident and reflected particles, *Geophys. Res. Lett.*, 8, 987, 1981.
- Bonifazi, C., P. Cerulli-Irelli, A. Egidi, V. Formisano and G. Moreno, The EGD positive ion experiment on the ISEE-B satellite, *IEEE Trans. Geosci. Elec.*, GE-16, 243, 1978.
- Candidi, M., S. Orsini, and V. Formisano, The properties of ionospheric  $O^+$  ions as observed in the magnetotail boundary layer and northern plasma lobe, *J. Geophys. Res.*, in press, 1982.
- De Coster, R. J., and L. A. Frank, Observations pertaining the dynamics of the plasma sheet, *J. Geophys. Res.*, 84, 5099, 1979.
- Fairfield, D. H., Electric and magnetic fields in the high latitude magnetosphere, *Rev. Geophys. Space Phys.*, 15, 457, 1977.
- Frank, L. A., R. L. McPherron, R. J. De Coster, B. G. Burek, K. L. Ackerson, and C. T. Russell, Field-aligned currents in the Earth magnetotail, *J. Geophys. Res.*, 86, 687, 1981.
- Lui, A. T., L. A. Frank, K. L. Ackerson, C.-I. Meng, and S.-I. Akasofu, Systematic study of plasma flow during plasma sheet thinnings, *J. Geophys. Res.*, 82, 4815, 1977.
- Orsini, S., M. Candidi, H. Balsiger, and A. Ghielmetti, Ionospheric ions in the near Earth geomagnetic tail plasma lobes, *Geophys. Res. Lett.*, 9, 163, 1982.
- Parks, G. K., C. S. Lin, K. A. Anderson, R. P. Lin, H. Renee, ISEE 1 and 2 particle observations of outer plasma sheet boundary, *J. Geophys. Res.*, 84, 6471, 1979.
- Peterson, W. K., R. D. Sharp, E. G. Shelley, R. G. Johnson, and H. Balsiger, Energetic ion composition of the plasma sheet, *J. Geophys. Res.*, 86, 761, 1981.

- Pilipp, W., and G. Morfill, The plasma mantle as the origin of the plasma sheet, in B. M. McCormac (ed.), "Magnetospheric Particles and Fields", 55, D. Reidel Publ. Co., Dordrecht - Holland, 1976.
- Rostoker, G., and Bostrom, A mechanism for driving birkeland current configuration in the auroral oval, J. Geophys. Res., 81, 235, 1976.
- Russell, C. T., The ISEE 1 and 2 fluxgate magnetometers, IEEE Trans. Geosci. Elec., GE-16, 243, 1978.
- Sharp, R. D., D. L. Carr, W. K. Peterson, and E. G. Shelley, Ion streams in the magnetotail, J. Geophys. Res., 86, 4639, 1981.
- Spieldvik, W. N., and T. A. Fritz, Energetic ion and electron observations of the geomagnetic plasma sheet boundary layer: three dimensional result from ISEE-1, J. Geophys. Res., 86, 2480, 1981.
- Williams, D. J., Energetic ion beams at the edge of the plasma sheet: ISEE 1 observations plus a single explanatory model, J. Geophys. Res., 86, 5507, 1981.

## FIGURE CAPTIONS

Figure 1 - Three dimensional plots of the plasma experiment count rates summed over the tailward flow sector (bottom) and over the earthward flow sector (top) versus energy-per-charge versus time, for event A. The energy per charge scale is logarithmic. The count rate scale is linear.

Figure 2 - Energy-per-charge spectra of the differential fluxes ( $\text{cm}^{-2} \text{s}^{-1} \text{sr}^{-1} \text{keV}^{-1}$ ) from the ISEE-2 plasma experiment (dots) and from the ISEE-1 ICE (circles for  $\text{O}^+$  ions and triangles for protons). The bottom panel represents the measurements taken in the tailward flow sector, while the top panel indicates the fluxes detected in the earthward flow sector. The data are averaged over one hour (0300-0400, day 114). Symbols drawn on the base line indicate that the flux is below the sensitivity threshold of the instruments.

Figure 3 - The first three plots (from the bottom) show the time dependence of the  $\text{O}^+$  beam parameters, (bulk flow velocity, thermal velocity perpendicular to  $\underline{E}$ , density) for the time period 2300 UT, day 113 to 0700 UT, day 114. The shading at bottom indicates that  $\text{O}^+$  is not observed or that its density is below threshold. The fourth plot shows the trend of  $E_z$ , the computed value of the north-south electric field. The ISEE-2 plasma experiment positive ion count rates, in the 5-10 keV range, and the ISEE-1 electron spectrometer data, in the 749 eV energy channel, are plotted in the top panels.

Figure 4 - A time sequence of four time contiguous angular distributions of a typical  $\text{O}^+$  ion beam detected by the ISEE-2 plasma experiment on day 114, 0312- 0317 UT during a plasma sheet-lobe boundary crossing, in a coordinate system  $v_x v_y$  SE. In this type of display all particles are attributed the same mass and equivalent  $\text{H}^+$  velocities are computed.

Every angular distribution is taken over 96 seconds. The colours are proportional to the log of the differential fluxes according to the scales on the right of the single panels. The light blue areas are the  $-34^\circ$  to  $+34^\circ$  solar ecliptic longitude tailward flow sectors in which the high angular resolution data are taken. The broken lines are the ISEE-2  $XY_{SE}$  magnetic field projections.

Figure 5 - Same as Fig. 1 for the two time periods of event B.

Figure 6 - Energy-per-charge spectra of the differential fluxes ( $\text{cm}^{-2} \text{s}^{-1} \text{sr}^{-1} \text{keV}^{-1}$ ) from the ISEE-2 plasma experiment and from the ISEE-1 ICE, as described in Fig. 2, averaged over one hour of event B (1800-1900 UT, day 100).

Figure 7 - Same as Fig. 3, for the  $O^+$  parameters (bottom), the computed  $E_z$  (middle) and the 5-10 keV ion count rates together with the 219 eV electrons, for the time period 1600 UT - 2300 UT on day 100.

Figure 8 - 3-D plots of the ISEE-2 plasma experiment data, as described in Fig. 1, for the two time periods of event C.

Figure 9 - Energy-per-charge spectra of the differential fluxes ( $\text{cm}^{-2} \text{s}^{-1} \text{sr}^{-1} \text{keV}^{-1}$ ) from the ISEE-2 plasma experiment and from the ISEE-1 ICE, as described in Fig. 2, averaged over the time period 0840-0940 of event C.

Figure 10 - Time evolution of the  $O^+$  parameters, of the  $E_z$  computed value and of the 724 eV electron count rates, as described in Fig. 3, for the time period 2100-2400 UT on day 104. During this period the 5-10 keV ion count rates are always at background in the ISEE-2 plasma experiment data.

Figure 11 - Results of the statistical analysis. From the left:  $O^+$  density,  $O^+$  bulk flow velocity and  $E_z$  histograms for plasma sheet (bottom), boundary (middle) and lobe (top) regions. The three right panels, from the bottom, represent the scatter plots of the  $O^+$  thermal velocity component parallel to  $\underline{B}$  versus the perpendicular component for the three regions. The top right panel shows the ISEE-2 orbit segments when the  $O^+$  beams have been detected. The thick line refers to plasma sheet and boundary regions, while the thin line indicates lobe regions.

Figure 12a - Four angular distributions (as described in Fig. 4) for the time period 1450<sup>44</sup> UT - 1452<sup>53</sup> UT, day 81, 1979. The top left is a complete scan in all directions of the differential fluxes from the ISEE-2 plasma experiment, in the 96 seconds normal operation mode (WES). The other three panels show the angular distribution in the tailward flow sector only for some selected energy channels (light blue areas), close to the maximum, in the high time resolution mode (HTR). Subsets of the available energy range are shown because of the absence of any signal in the other energies.

Figure 12b - Four angular distributions (see Fig. 4 for description) of the differential fluxes from the ISEE-2 plasma experiment for the HTR mode time period between 1453<sup>14</sup> and 1453<sup>29</sup> UT, day 81, 1978 and for the WES mode scan at 1500<sup>33</sup> UT.

ISEE-2 PLASMA EXPERIMENT

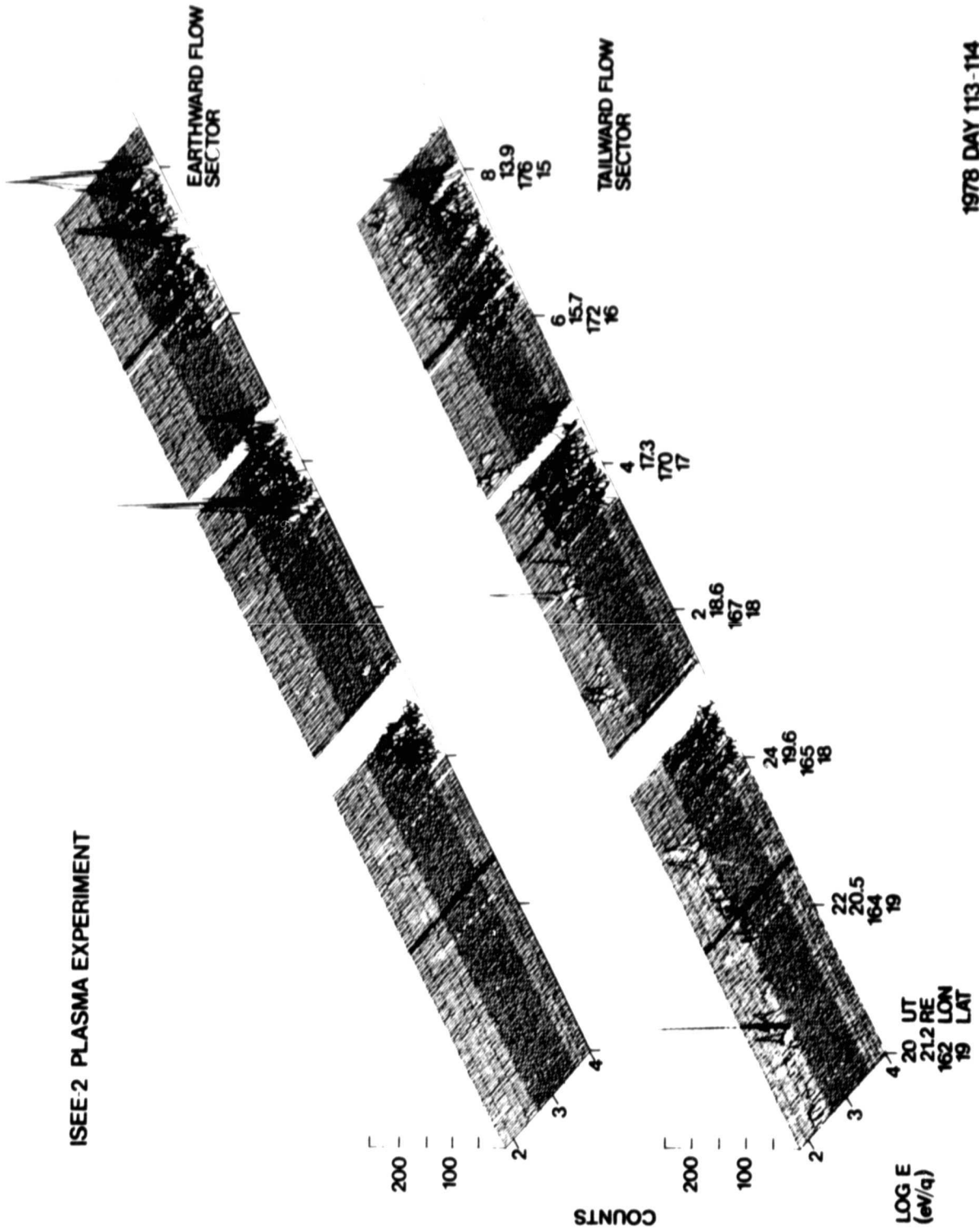


Figure 1

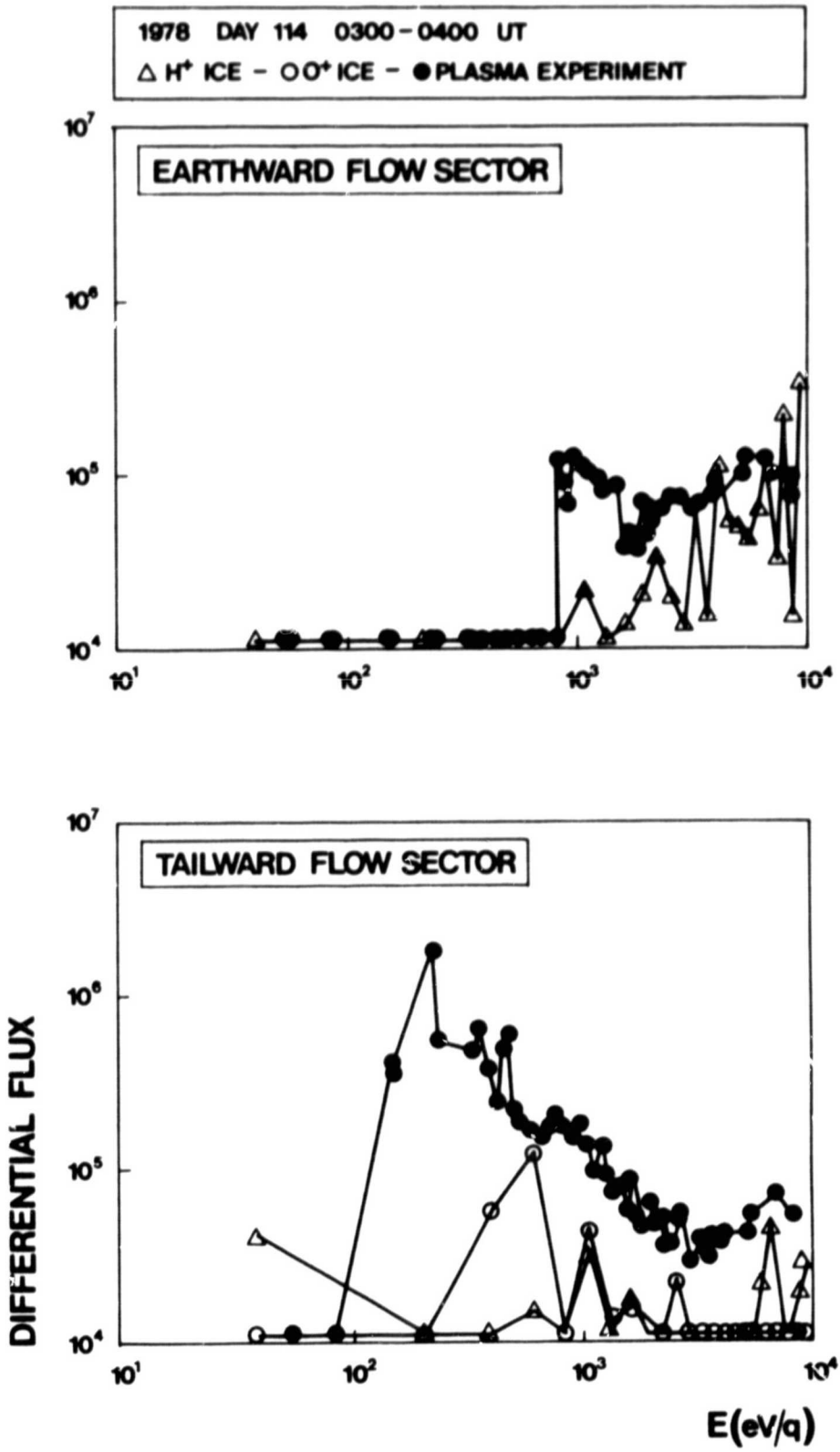
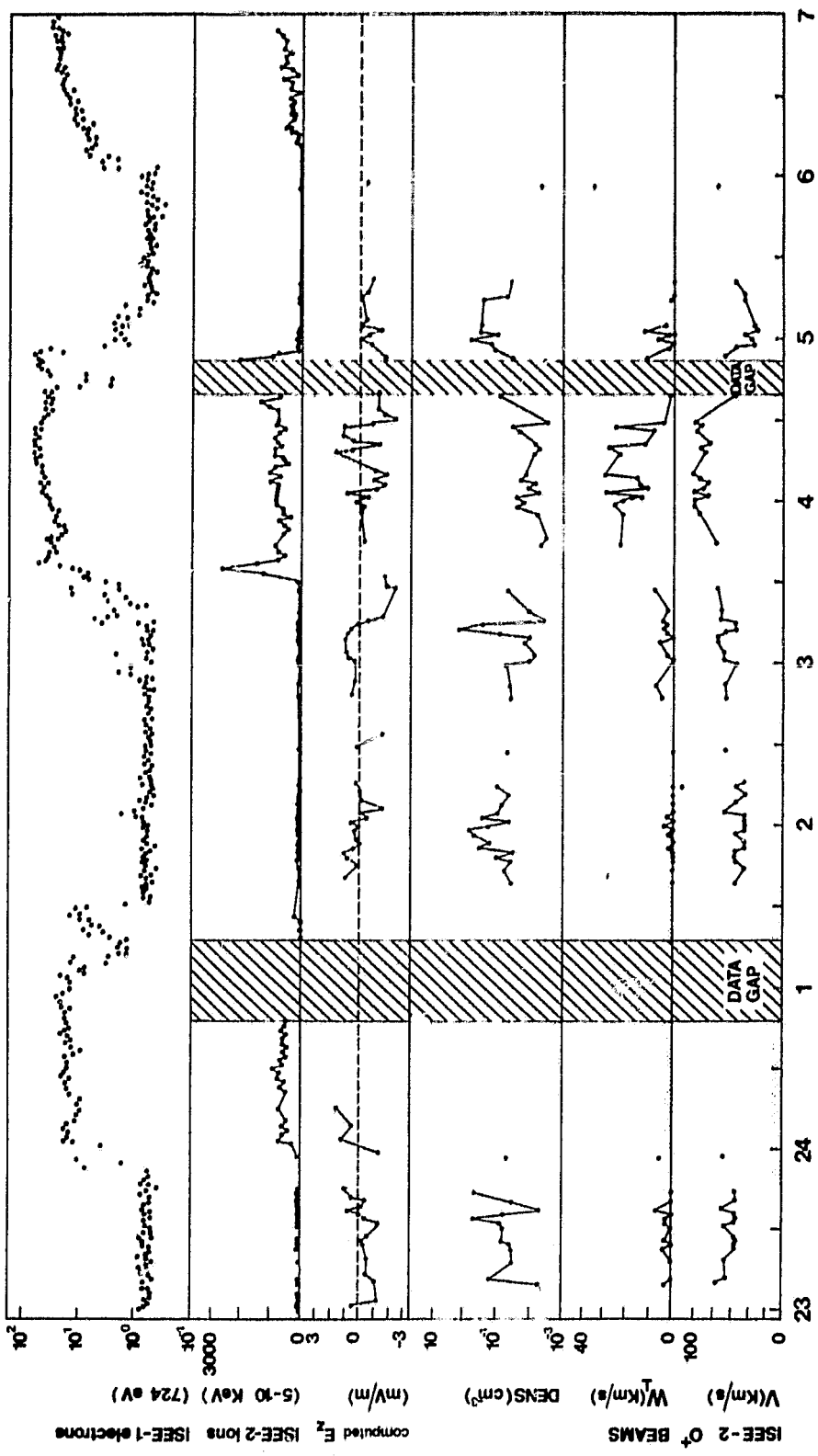


Figure 2



1978 DAY 113-114

Figure 3

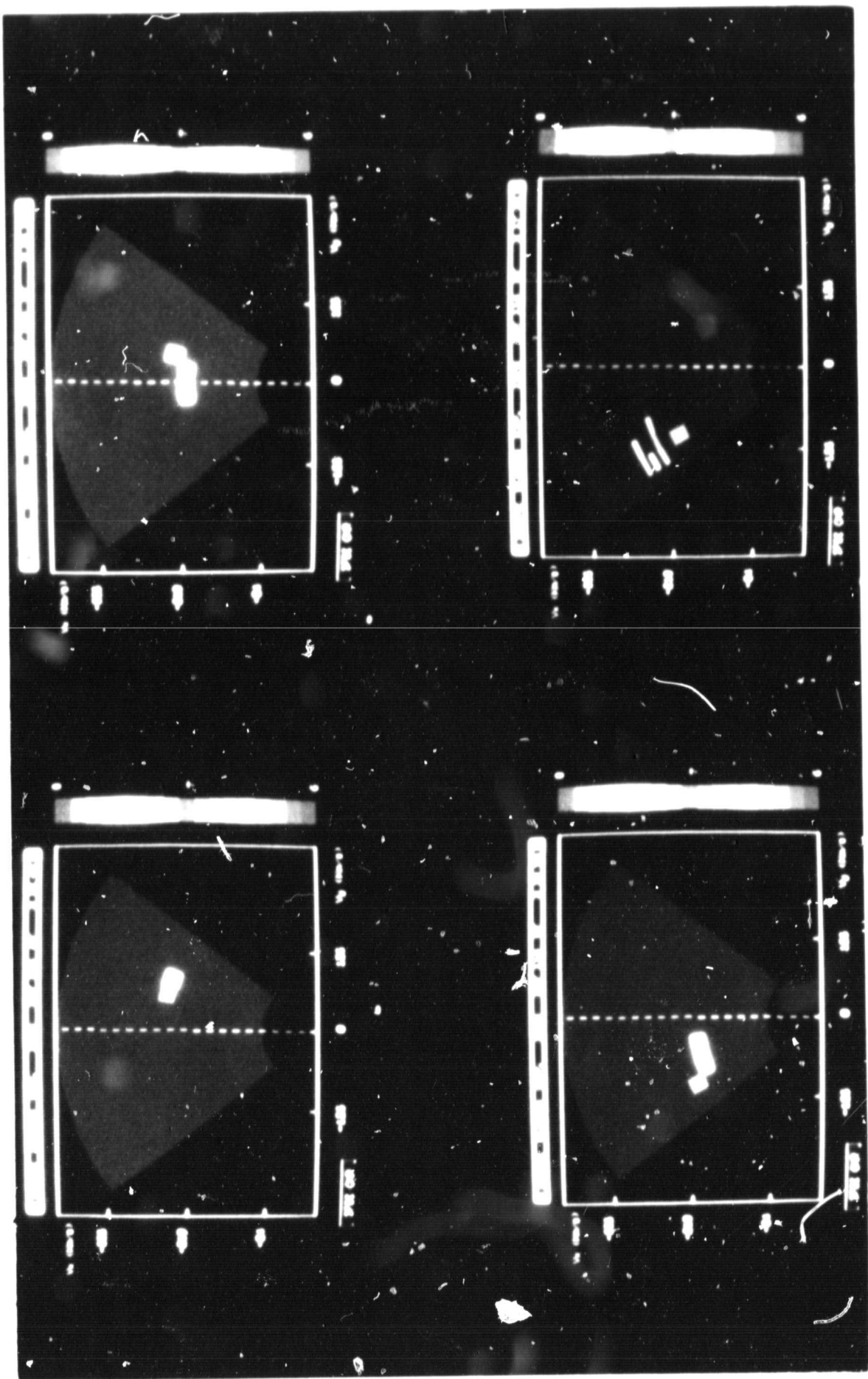
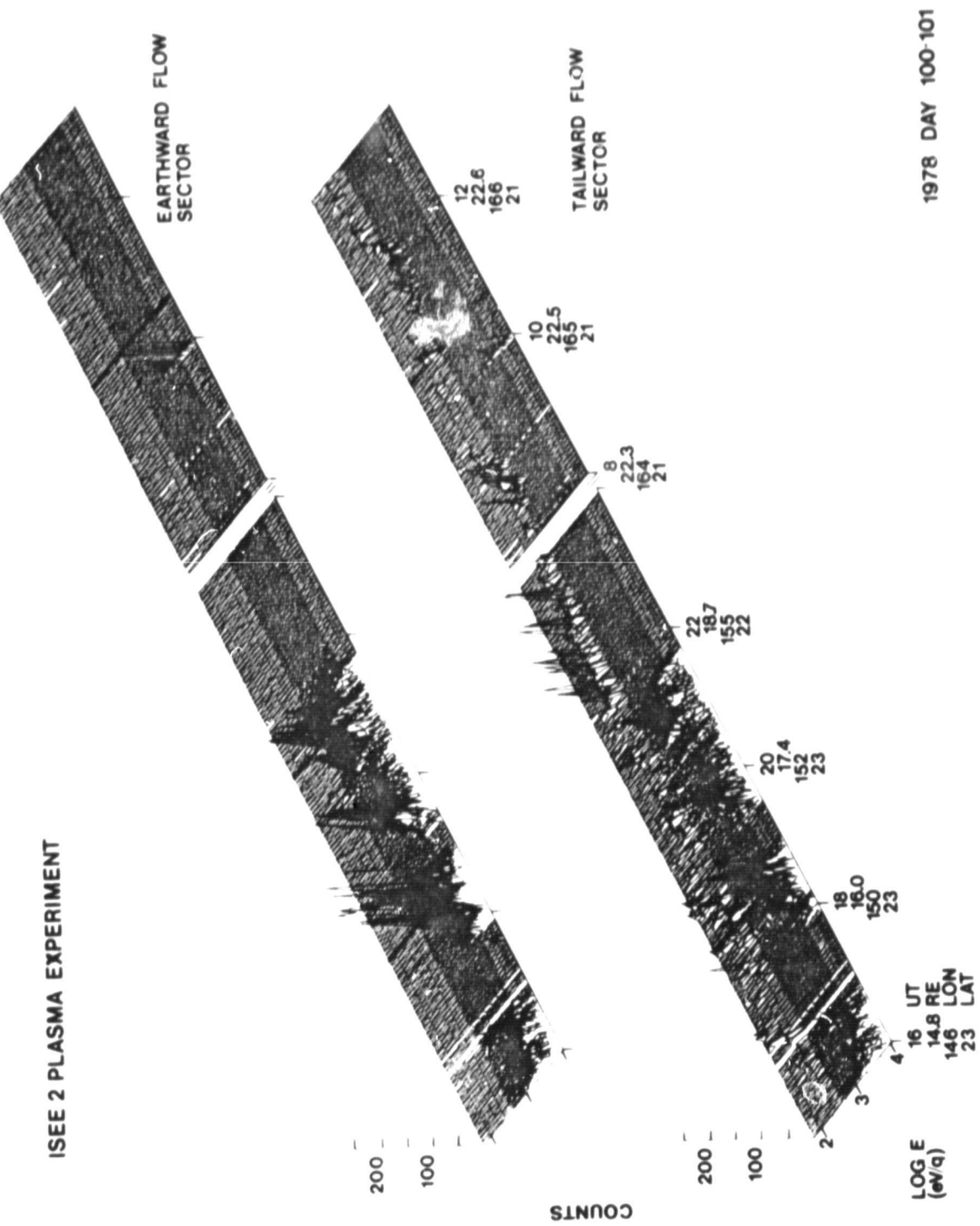


fig. 4

ISEE 2 PLASMA EXPERIMENT



1978 DAY 100-101

Figure 5

1978 DAY 100 1800 - 1900 UT  
 $\Delta$  H<sup>+</sup> ICE -  $\circ$  O<sup>+</sup> ICE -  $\bullet$  PLASMA EXPERIMENT

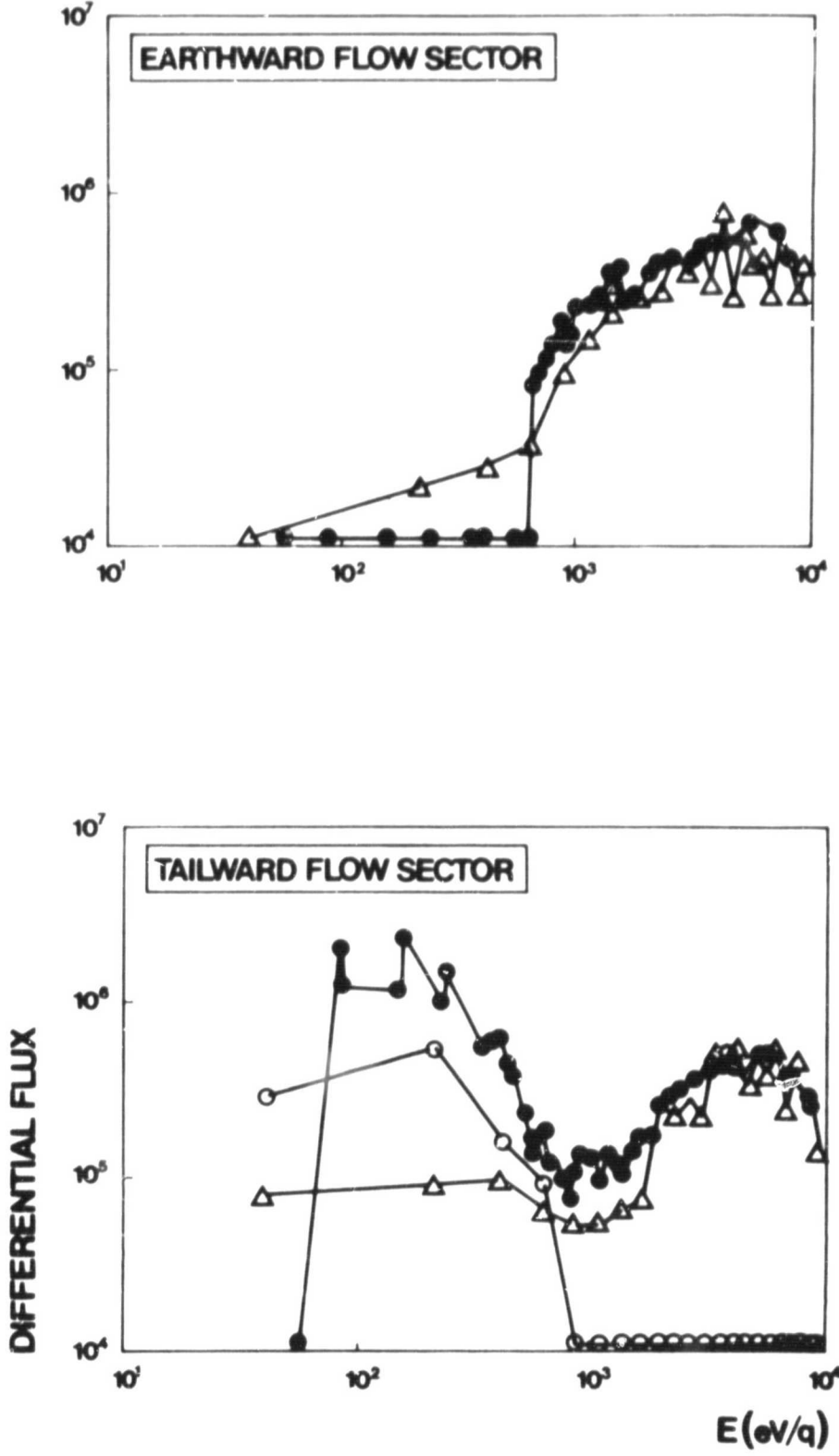
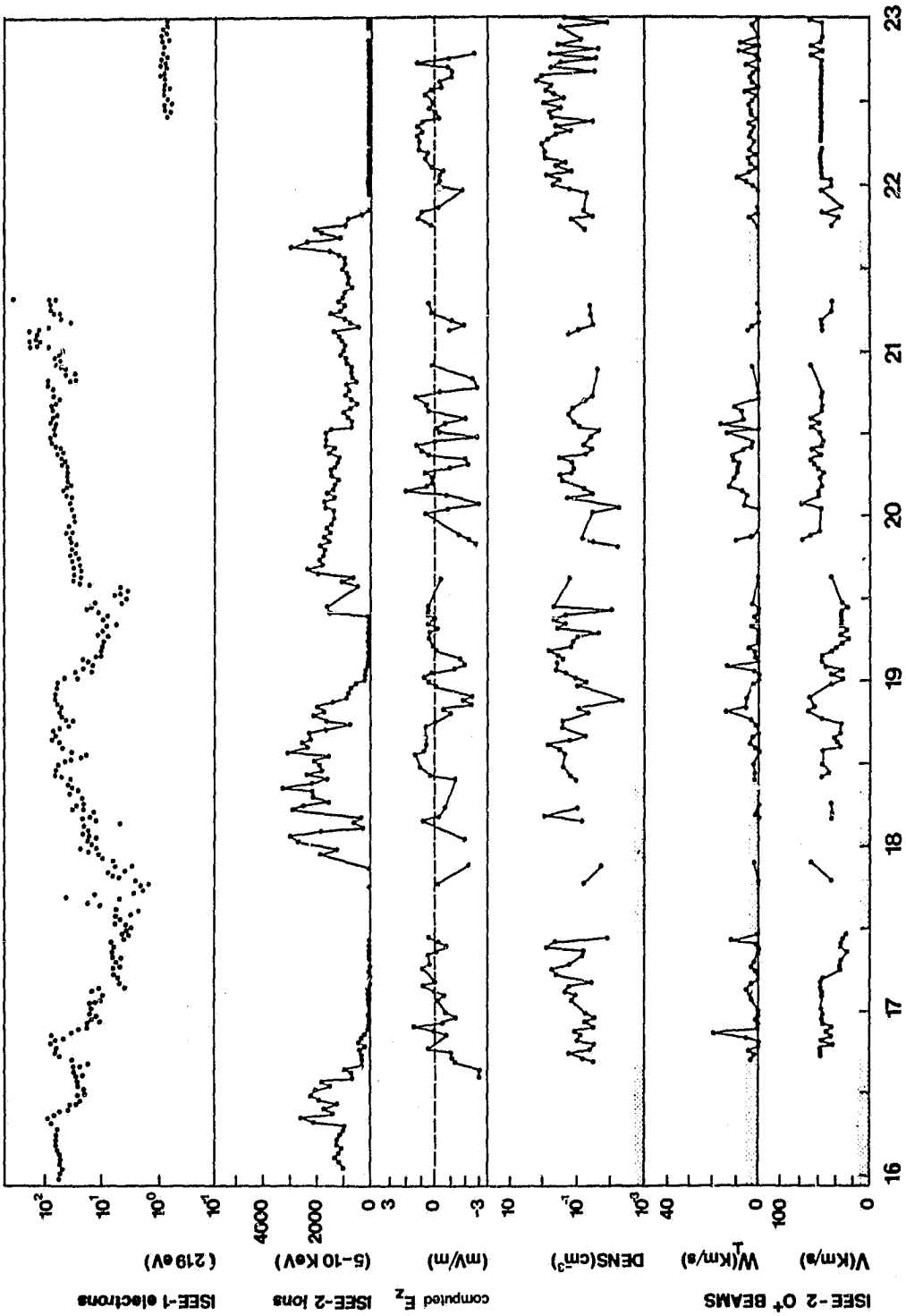


Figure 6



1978 DAY 100

Figure 7

ISEE-2 PLASMA EXPERIMENT

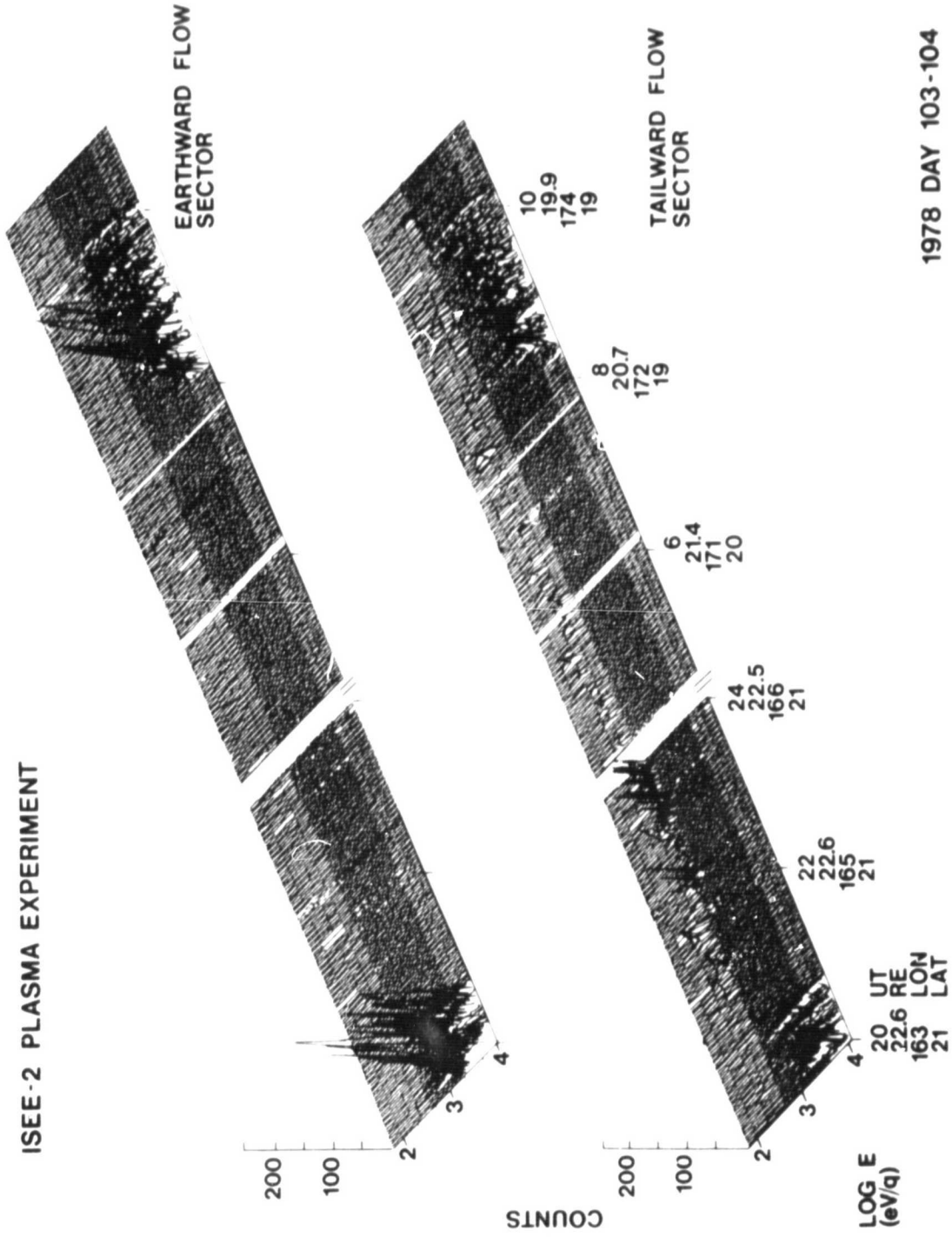


Figure 8

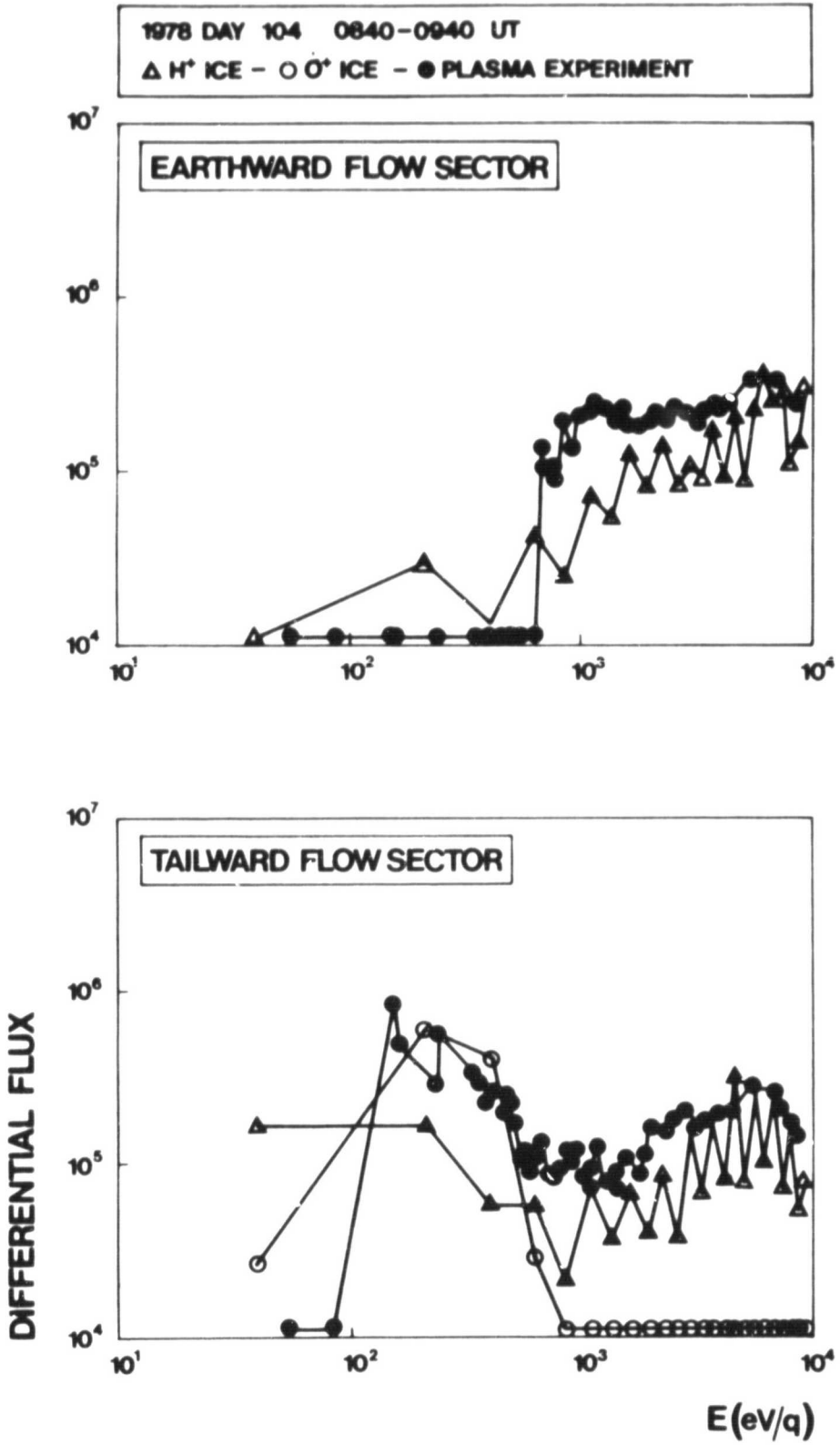
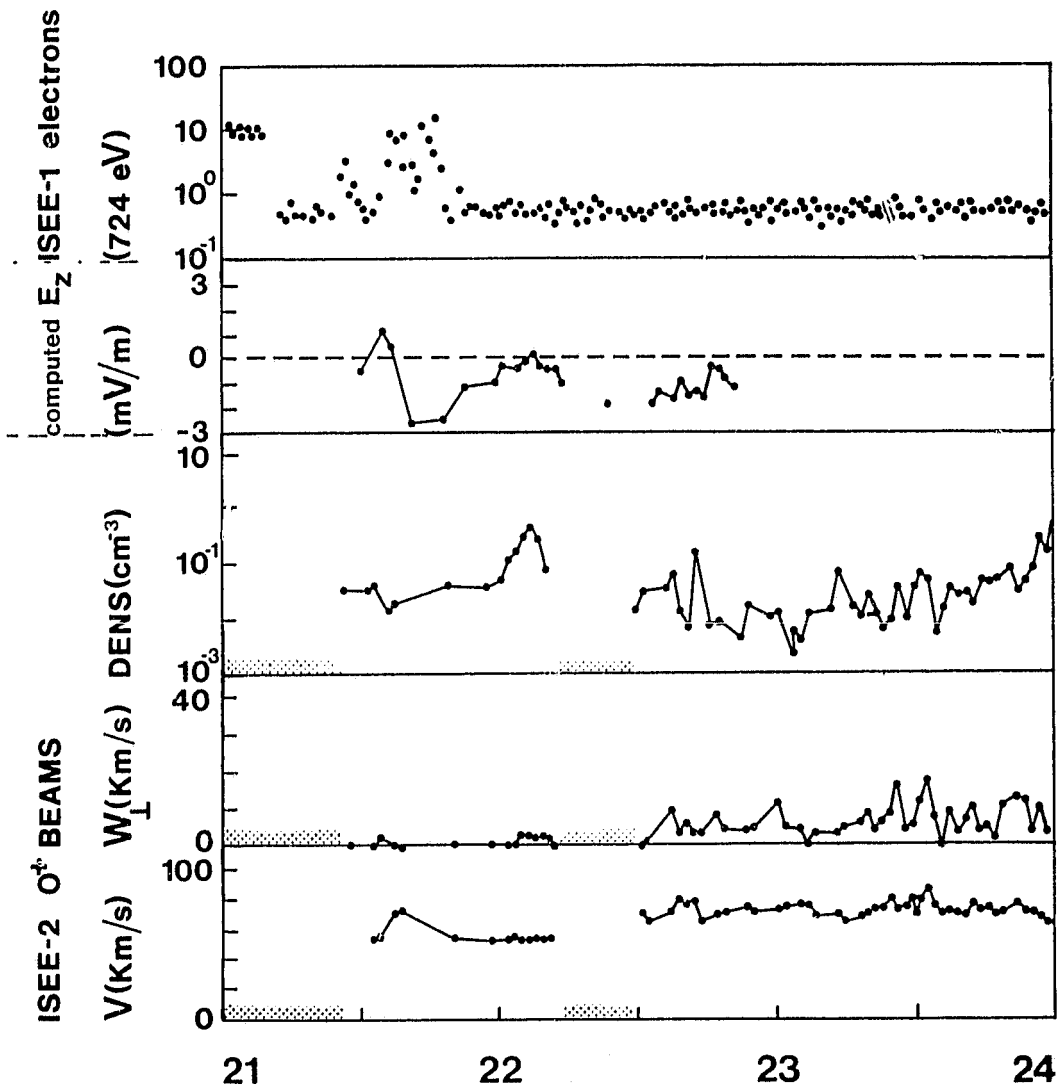


Figure 9



1978 DAY 103

Figure 10

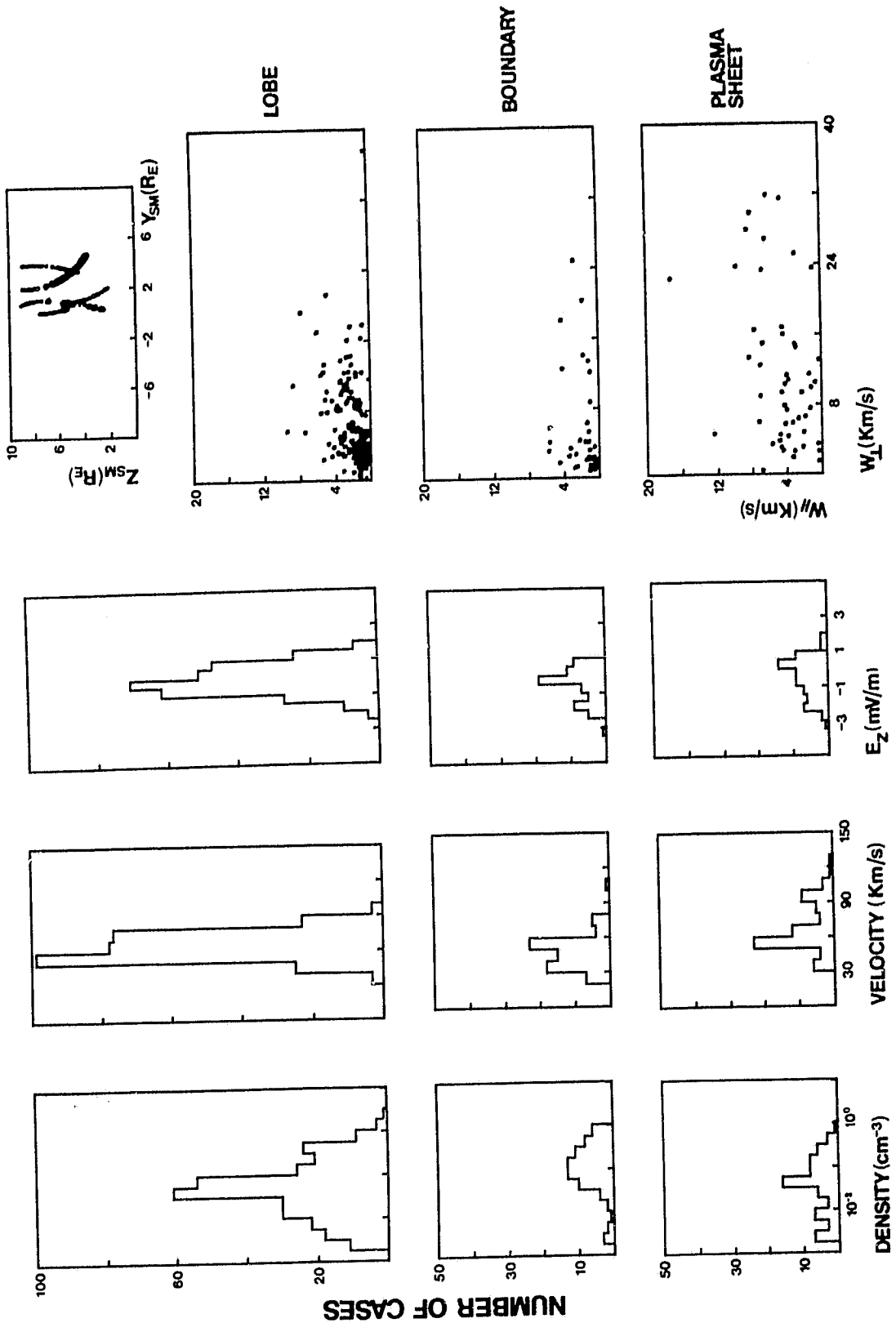
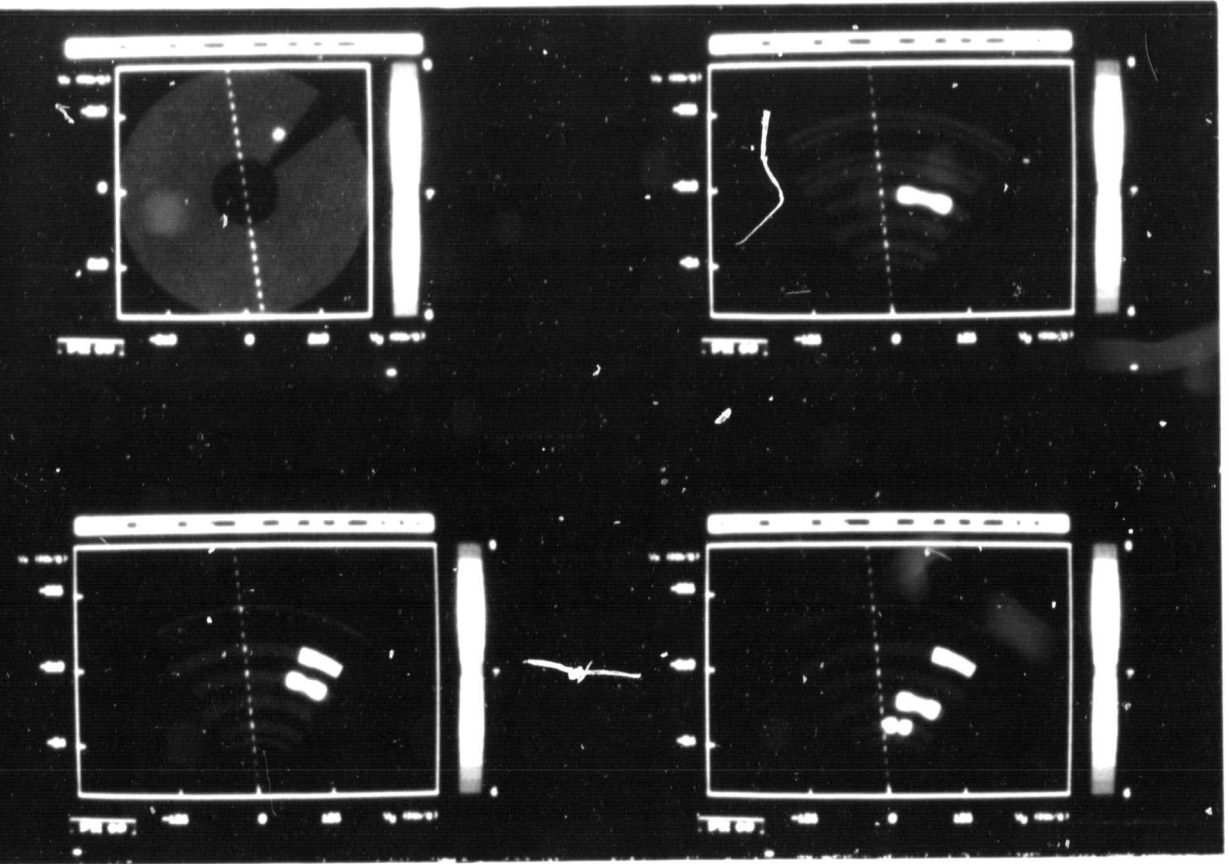
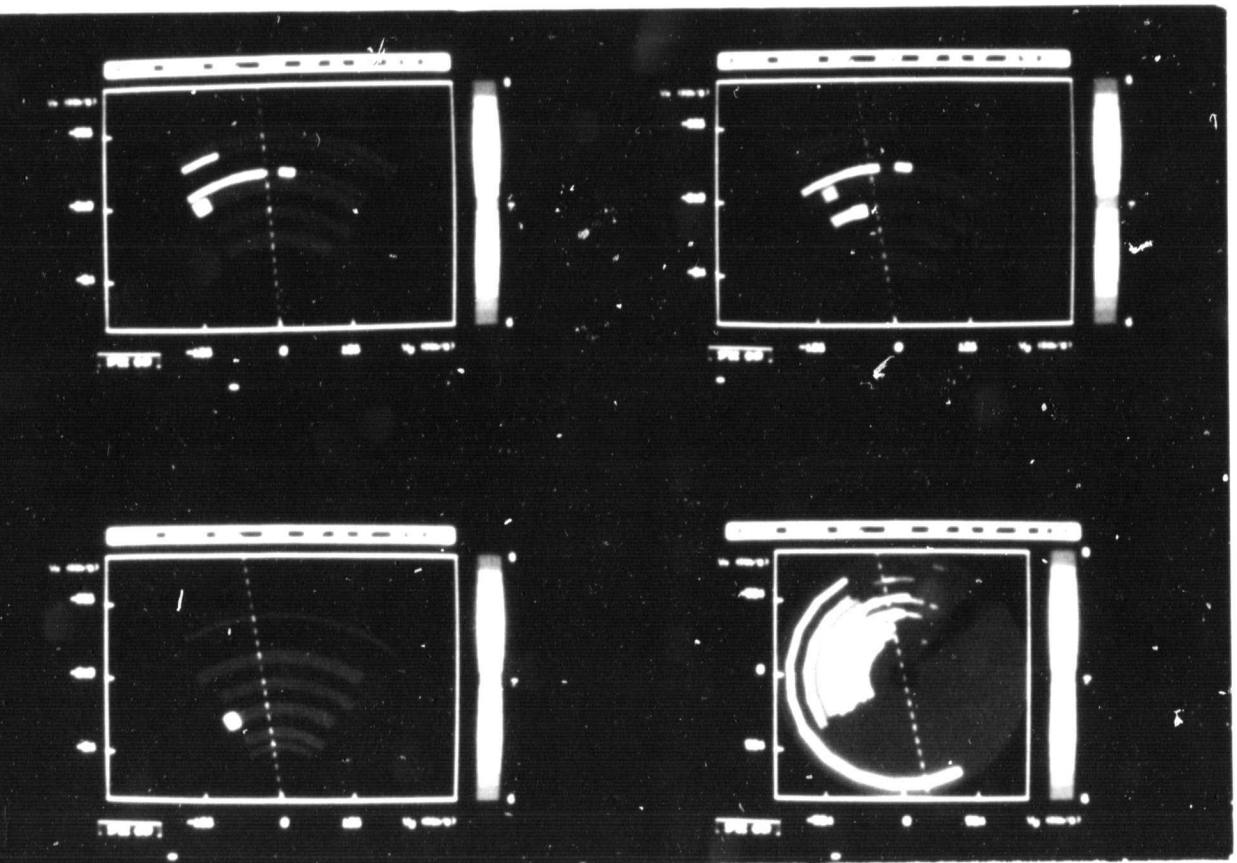


Figure 11



**fig. 12 A**



**fig. 12 B**